'*Carbon Nanotechnology*', Dai, L. (Ed.), Chapt. 6, p. 127-151, Elsevier: Dordrecht, **2006**.

Carbon Blacks as the Source Materials for Carbon Nanotechnology

Masaki Ozawa and Eiji Ōsawa*

NanoCarbon Research Institute, Toudai Kashiwa Venture Plaza, 5-4-19 Kashiwa-no-ha, Kashiwa, Chiba 277-0882, Japan

Contents

Abstract

The structure and formation/growth mechanism of soot particles (carbon blacks) have recently been elucidated by TEM experiments, and this study led to a surprising conclusion that the primary particles of carbon blacks are highly defective multi-shell fullerenes. The conclusion further led us to propose new synthesis of C_{60} by pyrolysis, and improved preparation of carbon nano-onions and nano- to submicron-diamonds, at very low cost. Smallest members of nano-onions are obtainable as by-products from the pyrolytic synthesis of C_{60}, and considered as the potential starting material for superhard carbons, Mackay crystals.

Keywords

Soot, buckminsterfullerene, C60, diamond, nano-onion, multi-shell fullerene, pyrolysis, Mackay crystal, schwarzite, hard carbon, furnace black

3. Introduction

If it were not for the discoveries of C_{60} in 1985 and carbon nanotube in 1991, coming of nanotechnology [1] may have been delayed by at least a few decades. The impact was so big that C_{60} and carbon nanotube continued to occupy major positions in the international research arena until long after the initiative in nanotechnology was taken over on national scales [2]. However, the problem of forbiddingly high production cost gradually caught up with the glory of fullerene carbons. A brief summary on the production cost of fullerenes and carbon nanotubes is given in the first four entries in Table 1. Even though the second-generation combustion method is supposed to improve C_{60}/C_{70} ratio to a very high level and to reduce the cost to one-tenth of the present level, $500/kg for the C_{60}/C_{70} mixture is still too high. HiPco method is so far the only practicable method of producing single-wall carbon nanotubes (SWCNTs) of acceptable quality in macroscopic quantities[2], but its price level is simply too high to seriously consider any industrial applications. The current cost level of $150/kg for producing multi-wall carbon nanotubes (MWCNTs) by chemical vapor deposition (CVD) method is certainly acceptable, but their application is rather limited [3].

Table 1 Production costs of major nano-carbon materials.

	starting materials	method	**products**	production costs ($10 /kg)	notes
1	hydrocarbons	**first-generation combustion method**	**mixture of C_{60}/C_{70} (6 / 4)**	500	40 ton /year under operation
2	hydrocarbons	second-generation combustion method	**mixture of C_{60}/C_{70} (>10)**	50	under development
3	CO/Fe	HiPCO	**SWCNTs + catalysts**	100,000	under test operation
4	hydrocarbons	CVD	**MWCNTs**	15	operation has started
5	carbonaceous industrial wastes	pyrolysis	**carbon blacks**	0.1	matured industry
6	carbon blacks	electron beam irradiation	**carbon nano-onions**	0.2	being planned
7	carbon nano-onions	electron beam irradiation at high temperatures	**nano-diamonds**	1.0	being planned
8	carbonaceous industrial wastes	pyrolysis	**C_{60},C_{60}@C_{240}**	0.1	being planned

We may have been pre-occupied by the too bright prospect of these fullerenes for too long. After a decade of continued failure in the search of better production methods, it is perhaps time to think of alternatives. The purpose of this Chapter is to shed light on the cost problem from a new angle. The central issue is to consider *carbon*

blacks, being produced on the very large scale all over the world, as the new source materials for carbon nanoparticles [4,5]. The proposal is based on our own work on the structure and formation mechanism of soot, which will be disclosed in some detail below, but the definitive advantage can be immediately understood by looking at the lower half of Table 1. Carbon blacks are prepared at a rate of $1/kg in high yield by pyrolysis of carbonaceous industrial waste like the distillation residue from the cracking of crude oil.

2. Review of soot and carbon blacks

Carbon blacks are the established industrial intermediates [2]. Taking a number of distinguished features including inexhaustible starting material, extremely low production cost, and almost perfect purity and homogeneity (Table 2) into accounts, we consider them qualified in the first requirement for the source material of carbon industry. Perhaps the readers are curious about the reason why one can produce such pure and uniform carbon at such a low cost. Before discussing the second requirement, which is a list of potential applications, we will briefly mention the production of carbon blacks, a topic rarely discussed recently.

Table 2 Characteristics of carbon blacks as industrial materials.

items	values	notes
carbon content	97 - 99 wt%	by-contents are H and O
bonding states of carbon	sp^2 carbon	high degree of purity
microstructures	bunched agglutinates of spherical primary particles	The less agglutinative for the larger primary particles
homogeneity of microstructures	100%	common feature in high temperature Pyrolysis
starting materials	carbonaceous industrial wastes	oil cokes or residual oil
production method	mainly furnace black method	fluidized continuous prolysis
production costs	~$1 /kg	stable
production /year	~10M ton	distributed plants in the world
products	black granulated powder	mainly used as reinforcement of rubber and black toner

Essentially carbon blacks are the pure soot, and produced by pyrolysis of carbonaceous industrial waster. The pyrolysis furnace, the core of the whole process, is a huge empty tube several dozen meters in length, ca. 2 m in diameter, and made of heat-resistant bricks as illustrated in Fig. 1. Coal gas or natural gas is mixed with air and the mixed gas introduced from one end of the tube, compression-ignited, and the high-temperature flame (1800-2000 °C in the highest case)

thus generated is blown at a supersonic flow toward the other end. A little downstream, carbon-containing industrial waste like oil cokes or residual oil, fluidized by preheating at 200–300 °C, is sprayed into the high-temperature current of flame to produce soot through cracking. When the soot thus produced grew to a desired size, water is sprayed in further downstream to extinguish combustion and suspend the cracking processes and the soot is gathered after cooling by passing through a long vertical pipe.

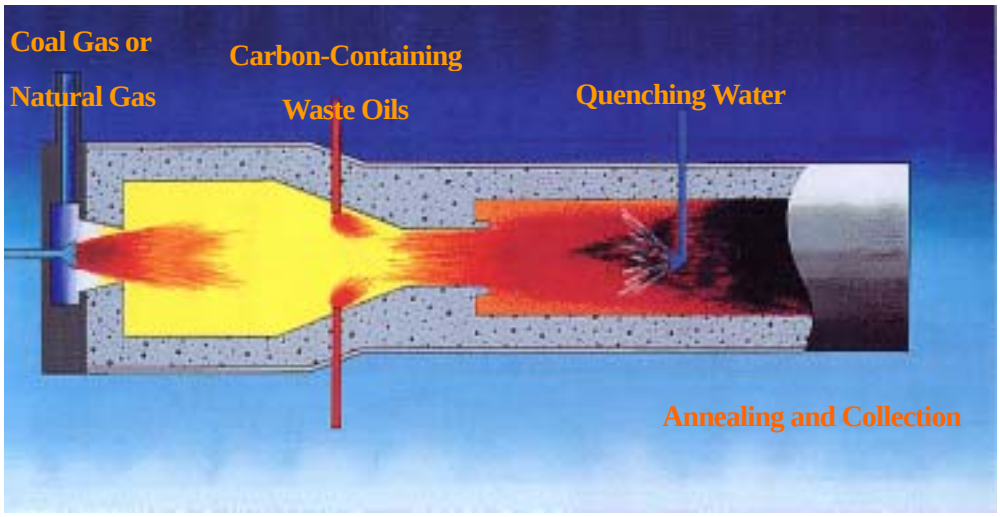

Fig. 1 Pyrolysis furnace for carbon blacks. Classical process produces chemically pure carbon which turned to be a sort of fullerene.

One should not misunderstand at this point the main sooting process as incomplete combustion of the starting materials. On the contrary, the combustion taking place in the furnace is complete

combustion of the fuel gas, and the role of high-temperature supersonic flow thus generated in the first segment of furnace is to supply heat for the cracking process of the industrial waste. The cracking reaction may appear quite simple, but the chemistry of soot formation involving self-assembly of the atoms or atomic fragments, clustering, network formation, and growth processes into soot particles is actually highly complicated. Only a rough picture has been indicated here [6].

The largest drawback of carbon blacks as industrial materials is the low crystalline nature: carbon blacks are categorized as amorphous carbon. Nevertheless, the application for the reinforcement of tires began at the beginning of the 20^{th} century and proved a great success. Demand for this single market grew rapidly with the expansion of vehicular transport. More than 10 million tons of carbon blacks are produced annually in automated plants all over the world [4, 5]. However, science of carbon blacks has remained almost 'black', even the structure of primary particles has defied elucidation for a long time until Rosalind Franklin presented a famous model based on X-ray diffraction analysis, wherein crystallites of graphite are assembled into turbostratic spherical structure [7].

Science of carbon blacks revived after the discovery of C_{60} at the end of 20^{th} century [8]. Our work on the mechanism of C_{60}

formation led us to the problem of soot structure, and by luck we could reveal all the basic aspects of structure and formation mechanism of primary soot particles [7]. As our present proposal is based on this fundamental study, the next section is devoted to its brief summary.

3. The structure and formation mechanism of carbon blacks

3-1. Crystallization of carbon blacks without heating

When a large number of molecules or atoms are ordered into 3-dimensional arrangements, chemists call the states as crystals. The better crystallinity generally gives the higher melting point and the less pronounced defects. On the other hand, material scientists say “crystals” or “with good crystallinity” even for partly ordered arrangements in bulk materials. The latter case will be followed for these terms in this chapter.

High-resolution transmission electron micrographs of carbon blacks generally display very low crystallinity as shown Fig. 2*a*. Although the average diameter of the primary particles in this photograph is given as 14 nm by the producer, it is clearly difficult to reach this number from this picture alone. It is naturally desirable to increase the crystallinity.

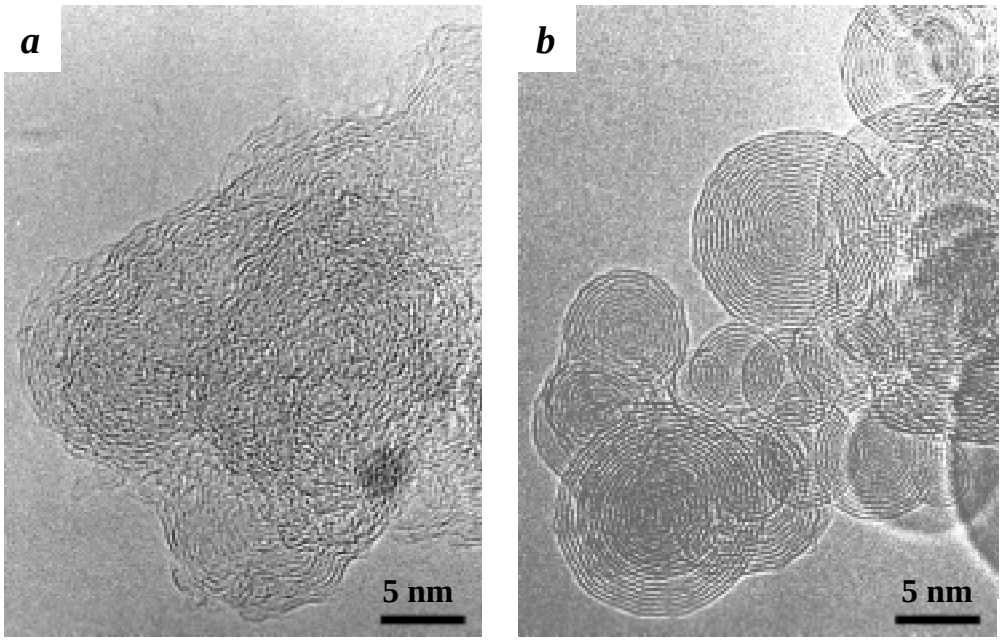

Fig. 2 Crystallization of carbon black structure by intensive electron beam bombardment (JEOL, JEM-2010 at 200 keV, ~150 A/cm2) onto Toka Black #8500F, claimed to have an average diameter of 14 nm in the primary particles. *a*) Pristine structure shows numerous defects and ambiguous grain boundaries. *b*) After irradiation for 20 min at this spot spherical contours and inner-layers of carbon nano-onions clearly appeared.

We find that primary particles of carbon blacks can be converted into carbon nano-onions upon irradiation with electron beam focused to a current density as high as 150 A/cm^2 in a high-resolution transmission electron microscope (HRTEM) [6]. The experiments are quite similar to those carried out by Ugarte originally using polyhedral carbon nanoparticles as the target [9]. Ugarte refers in his paper [9] to his preliminary experiments on amorphous carbons including carbon black, but it seems that he did not have much luck in

this direction. We later observed that carbon black samples with low crystallinity often fail to produce clear-cut conversion into nano-onion but decompose into undefinable structures. We were lucky enough to have started with the right sample having rather good crystallinity. The major factor responsible for such morphological modification in microscopes is the knock-on effect [10] of the electron beam. Hence, an acceleration voltage high enough to displace carbon atoms from the lattice is necessary for the nano-onion structure to improve.

The micrograph of nano-onions in Fig. 2*b* demonstrates the following characteristics:

(1) Larger nano-onions have more structural defects than smaller onions, which appear to have almost perfect structure.

(2) The outermost graphitic layers extending over more than one primary particle appear to have been mostly removed under electron beam irradiation, while some of the extended layers still remain in this picture.

(3) The innermost shell is C_{60}.

(4) Some particles have spiral layers instead of concentrically nested ones. A spiral image with 12 nm in diameter located in the upper center of Fig. 2b provides an example of non-onion particle, a spiroid.

3-2. Discovery of spiroid intermediates

An astonishing phenomenon was then observed, when electron bombardment was kept going longer time in order to achieve conversion into perfect nano-onions: every primary particles of carbon blacks always metamorphose to spiral intermediates during the structural evolution into nano-onions. In addition, the transformation between a spiral intermediate and a nano-onion is reversible as shown in Fig. 3, and sometimes occurs repeatedly with gradual change of the contour.

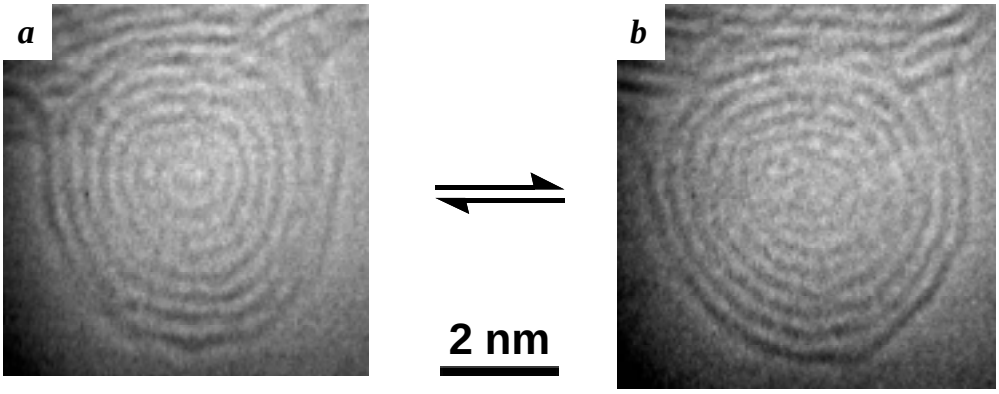

Fig. 3. Reversible transformation between the intermediate spiral particle (spiroid) *a*) and the carbon nano-onion *b*) observed under electron beam irradiation onto primary particles of carbon blacks.

Carbon nano-onions are in general spherical, and their centers filled. However, it is known that the shape changes at high

temperatures into faceted polyhedral nanoparticle, often with void in the center [11]. Similar 'carbon nanoparticles' are also formed as by-products, when fullerenes are produced by the arc-discharge method. Polyhedral carbon nanoparticles are presumed to be more stable than spherical carbon nano-onions. However, the premise has never been proven experimentally because of the difficulty in isolation and purification of these nanoparticles.

On the other hand, it has been suggested by theoretical calculations that one particular onion series, $C_{60}@C_{240}@C_{540}@C_{960}@C_{1500}@\cdots\ @C_{60n^2}@\cdots$, is exceptionally stable irrespective of the number of layers, n, among large number of other homologous series [12]. In this series, inter-shell spacing is always nearly equivalent to those of graphite, and moreover, each giant fullerene shell takes the most stable π-electronic structure. It is likely that the spiral intermediates observed here are used for attaining this ideal structure.

The most difficult part of the present proposal was to conceive an acceptable molecular model of the spiral intermediates. The term "spiral" generally refers to a path of a point on a plane winding around a fixed center point with continuously increasing distances from it, and does not fit to 3-dimensional spherical shapes. At first a path of a semicircle winding around a fixed axis was examined, but we soon

realized that exact Archimedean spiral projection produced high strain along the rotation axis. We eventually found that a discretely growing arc, where the height increases with the rotation angle and the width increases at every 2π rotation, gives a more convincing structure.

A three-dimensional spiral molecular model of a carbon nanoparticle with a spiral projection thus generated contains discontinuous points, which are assigned to free radical centers. Additional free radical centers exist at the innermost and outermost ends of the spirals. These radicals are all stabilized by delocalization with conjugated carbon network (Fig. 4). Such hypothetical species were given a temporary name of "spiroids". Spiroid-to-onion transformation may occur if one assumes interlayer valence isomerization involving delocalized radical centers to propagate radially in a zipper-like fashion (Fig. 5) [6]. The series of spiroid-to-onion transformation must constitute a large exothermic reaction as a whole. Under constant input of large electron energy the reverse series of valence isomerization, namely the zipper-like onion-to-spiroid transformations will occur, probably assisted by the release of strain energy.

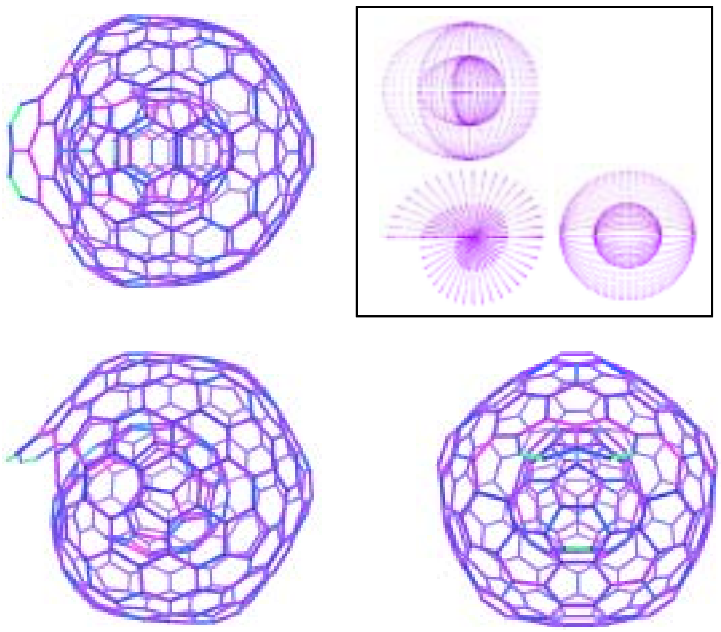

Fig. 4 Molecular and numerical (inset) models of a 3-dimensional double-layer spiral particle (spiroid), C300.

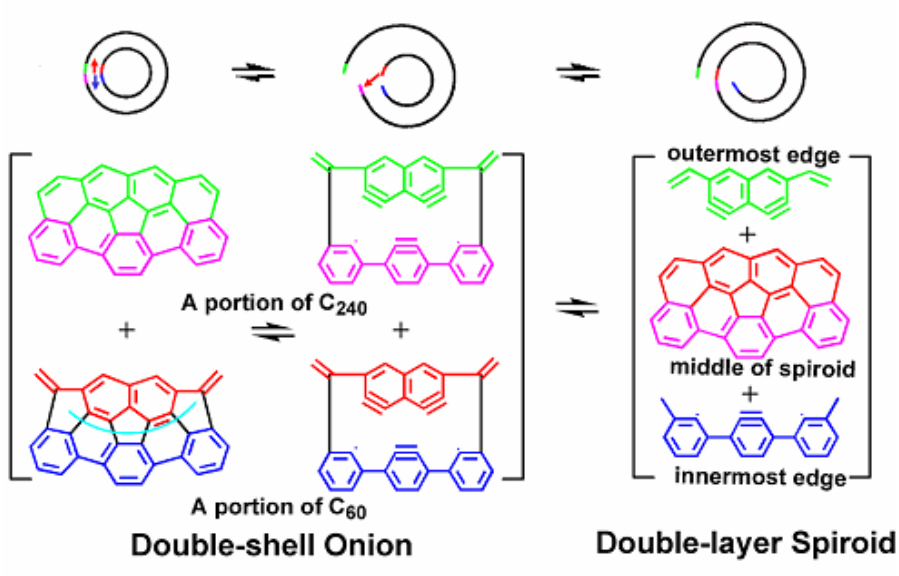

Fig. 5 Presumed reaction scheme of the reversible transformation between a double-layer carbon spiroid, C300, and a double-shell carbon nano-onion C60@C240. Cleavage of onion-shell starts at weak C-C bonds at structural defects, fused pentagons, etc., and prompts interlayer valence-bond isomerization.

3-3. Formation of carbon nano-onions and Homann mechanism

According to our mechanistic assumption, onion shells achieve the most stable structures from inside towards outside by repeating reversible spiroid-to-onion and onion-to-spiroid transformations accompanied by in-plane valence isomerization like Stone-Wales rearrangements. Carbon nano-onions and nanospiroids are likely to give the idealized models of primary soot particles, which have been a long-pending problem. It is exciting to realize the fact that soot, with which human-beings have been so familiar since they discovered fire, is a sort of fullerene.

Previously, Kroto [8] and Homann [13] studied the mechanism of fullerene formation in flame. Kroto's mechanism, called icospiral nucleation process, is the closest to ours, but he apparently thought of logarithmic rather than Archimedean spiral, and did not suggest any reasonable connection between spiral and onion structures. Homann intensively investigated the relationship between soot and fullerenes experimentally for ten years since 1987 when he found C_{60} in combustion flame of hydrocarbons. At the end of his career, he proposed a new mechanism of fullerene formation in soot, wherein the small unidentified species from pyrolysis of carbonaceous fuel grow through a series of well-identified species: polycyclic aromatic hydrocarbons (PAHs), their syn-dimers, and then fullerenes

by intra-dimer cyclization (Fig. 6). It is assumed that buckminsterfullerene C_{60} is formed only when the *syn*-dimer contained sixty carbon atoms. Dimers of PAH that do not give rise to C_{60} grow to oligomers by adding more PAH molecules, and eventually become soot. Negatively charged aromatic oligomers (aromers) including those having sixty carbon atoms have been identified by mass spectrometry. His scheme considered only the single-shell fullerenes like C_{60}.

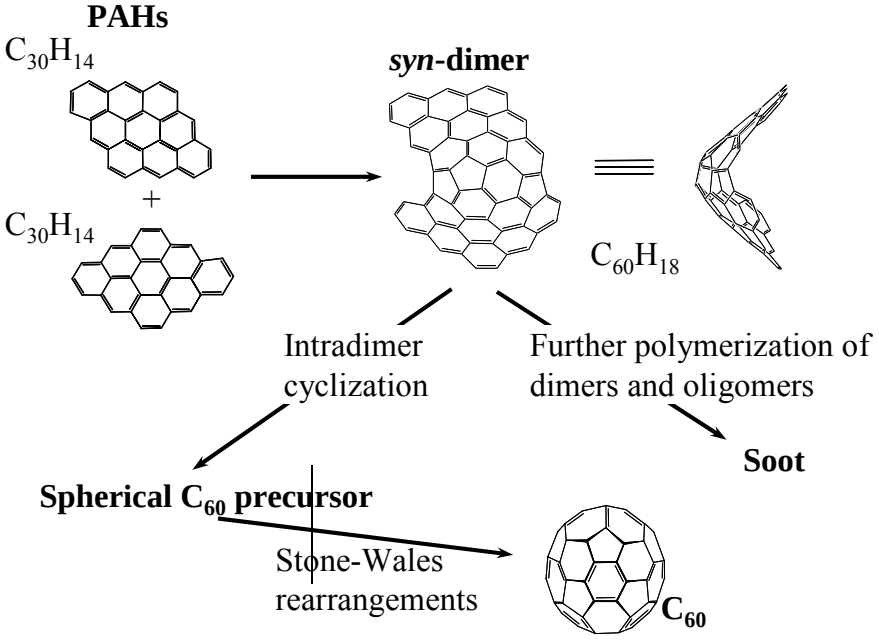

Fig. 6. Chemical transformations in the incomplete combustion process of hydrocarbon proposed by Homann. The first intermediates PAH polymerize into *syn*-dimer and other oligomers (aromers) but only the syn-dimer of thirty-carbon PAH is transformed into C60, while all the other aromers grow into soot.

3-4. Unified mechanism of soot and fullerene formation

We believe that syn-oligomerization of a discretionary pair of PAHs should be much more likely initiation process of primary particle formation than Homann's intramolecular cyclization of syn-dimers (Fig. 7). Subsequently, the products undergo reversible spiroid-onion transformation involving in-plane rearrangements under the high-temperature conditions. Continuous rearrangement process leads, like adamantane rearrangement [14], to thermodynamically the most stable $60n^2$ (n=1,2,3···) configuration of the infinite carbon nano-onion series with C_{60} (n=1) in the centre. Thus, concomitant formation of soot particles and fullerenes can be understood within the framework of a single collective mechanism. Single-layer fullerenes are formed only when syn-oligomerization of PAH happened to lead to closure to a spherical polyhedral solid during the first spiral turn. Even in such a case, total number of carbon atoms will be adjusted by the one-layer version of onion-spiroid transformation. Otherwise, continuous *syn*-addition of small carbon radicals, such as C_2, PAH, and aromer radicals onto the radical terminal at the outermost layer of spiroids lead to primary particles of soot.

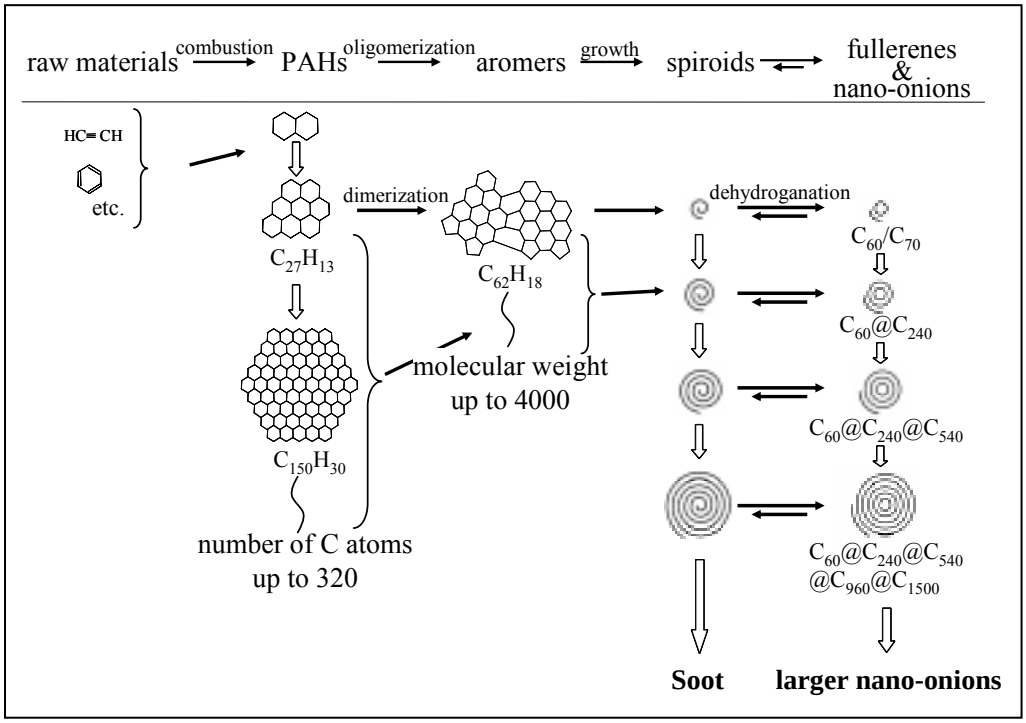

Fig. 7 Unified mechanism of formation/growth of soot, C60 and nano-onions. Some PAHs and only one aromer out of numerous structures are depicted as examples.

3-5. Secondary structure of soot by agglutination of primary particles

Chemistry of soot is complicated by the appearance of the secondary structures, or so-called 'aggregate' superstructure of the spherical primary particles (Fig. 8). Let us speculate on how the superstructure evolves. Primary particles may have been well-dispersed immediately after explosion and their formation, but the particles become aggregated as the pressure and temperature decrease, depending upon the size of particles (the smaller the

particles, the higher the tendency to aggregation). Under the incomplete combustion conditions of furnace black processes, concentrations of C_2, PAHs and aromer radicals are abundant at this point and the radical addition process continues at the outermost layer on the surface of aggregate to form deformed graphene layers extending over the entire surface of aggregate. As the aggregation and radical addition proceed simultaneously, the product will have complex structure, in which deformed graphene layers will be found not only on the surface but also in the inside of aggregates.

Fig. 8 Model of core agglutinate of a high-structure carbon black. Primary particle are believed to contain C60 or its congener in its centre. Outer layers are merged into large deformed and defective graphene sheets that hold the assembly of primary particles which are highly defective multi-shell fullerenes or its spiroidal counterpart.

The deformed graphene layers that bind primary particles together by both physical and chemical forces will be much more

resistant to weak perturbations like strong agitation than aggregates simply bound by van der Waals attraction force alone, but tend to break down readily by high-energy treatments with strong oxidants or even special mechanical impacts because of the abundant structural defects. It would be interesting to correlate the curvature properties of deformed graphene sheets with chemical and mechanical stability.

An important aspect of the above speculation is about the definition of aggregation. The word aggregation has been used primarily to the mass of particles assembled through physical force, namely *van der Waals* attraction. *Van der Waals* force is generally weak, and such aggregates can be easily dispersed by giving physical perturbation like grinding and mixing. On the other hand, forces that bind particles together within the 'aggregate' structure of carbon blacks are those of chemical bonds, hence the current terminology of using the same word of aggregation to two different kinds of assembly is confusing. For this reason, we suggest to call chemical aggregates as 'agglutinates' [15].

4 Carbon blacks as industrial materials

With the knowledge on the formation mechanism and on the structure of primary as well as secondary particles of carbon blacks, we now have some perspectives on their potential as the carbon

materials.

Crystallinity. The most outstanding defect of carbon blacks as the industrial carbon source is their low crystallinity. How can we improve the degree of crystallization? In the past heating has been traditionally used to increase crystallinity of poorly crystalline or amorphous carbons. The process is also called graphitization because graphite was the goal of the highest crystalline carbon. Now that fullerenes are recognized as another crystalline form of carbon, which attains stability due to the closed structure and favorable disposition of pentagonal defects, we have a new strategy to increase the crystallinity of non-graphitizing carbon: to convert carbon black into the most stable isomer of corresponding fullerene analog. In our case, the goal is carbon nano-onion with $60n^2$ (n=1, 2, 3···) configuration.

Heating strategy has long been adopted to carbon blacks by heating carbon blacks above 3000°C [4, 5]. The products of heating have been commercialized under the trade name of 'graphitized carbon black', but without much success. In our opinion, this is because the agglutination remained unchanged in the graphitized carbon blacks, even though primary particles were changed into giant polyhedral multi-layered fullerenes with void in the centre. Thus, the results of heating sharply contrasts with those of electron-beam irradiation (Fig. 2), wherein agglutination are destroyed and primary

particles are crystallized into nano-onions without any void.

Annealing of carbon black at high-temperature is much slower process than irradiation of high-current electron beam to give different products. Clearly the polyhedral particles with pentagonal defects aligned vertically to absorb uneven interlayer steric interactions are more stable than the carbon nano-onion where interlayer steric energy is absorbed by skeletal deformations to a sphere. Situation is much less clear about the fate of deformed outer layers under these two different modes of annealing; the slow heating probably crystallized the outermost layers as well, which should then become more resistant against destruction. On the contrary, rapid absorption of high-density electron beam at the surface of agglutinate must have led to destruction rather than crystallization.

Only the high-density electron beam is mentioned, but high-energy beams of atoms like proton and carbon should give similar but more pronounced effects compared to the former.

Dispersity. If we succeed in isolating carbon nano-onions or any other form of multi-shell fullerenes from carbon black, it would be the highest concern to keep them dispersed in order to appreciate the effect of nano-sized primary particles to full extent. The problem and countermeasures will be discussed elsewhere [16] .

Homogeneity and uniformity. Even though the structural

homogeneity of carbon blacks is almost perfect (Table 1), the structure itself is of low crystallinity. Furthermore, the nanostructure of carbon black is not uniform, consisting of highly defective primary particles and deformed outer layers on the surface of agglutinates.

5. Production of carbon nano-onions from carbon black

We found that irradiation of convergent electron beam onto carbon blacks leads to remarkable improvements in the crystallinity of the primary particles and at the same time to disintegration of agglutinate structures (Fig. 2). This novel transformation, listed in the 6^{th} row of Table 1, deserves more attention and will be analyzed in some detail in this section.

In spite of the characteristic structure equivalent to multiwall carbon nanotubes (MWCNTs) with zero length, carbon nano-onions have never been isolated in macroscopic amounts, impeding physical or chemical characterization of bulk or dispersion properties. However, their atomistic structures are well-investigated by calculation [12], and their bulk forms have often been observed under electron microscopes [9]. All the shells in a onion structure are akin irrespective of its size. In this regard, a mixture of nano-onions having a size distribution is similar to homologous mixtures of hydrocarbons like kerosene and gasoline. Nano-fractionation of the particles according to diameter

must be a challenging subject, once they are isolated.

Why cannot we apply the focused electron beam upon carbon blacks to isolate carbon nano-onions? This is simply due to the technical reason, that electron beam sources with large apertures working at high voltage and high density comparable to 200 keV and 150 A/cm^2, respectively, was not available. We knew the method of isolation, but the tool was missing. In this regard, carbon nano-onions were no more than painted delicacies. However, currently such a super-electron gun is gradually gaining reality. It has been already known since 1966 when the explosive electron emission was discovered in Russia by Mesyats/Fursey that high-density pulse electron beam is producible up to 1 MA/cm^2 even under the condition of low voltages [17]. A prototype of explosive electron emission devices was first produced in 2002 in Japan, by Uemura, and appeared on the market from Nagata Seiki Co., Ltd. in the following year under the commercial name of 'Corrosion Resistant System' (for metals) [18-19]. Irradiation of pulsed electron-beam of ultra-high density under a relatively low acceleration voltage of 20 keV upon metallic objects like metal mold quickly produces polishing effects. Despite large irradiation area of about 100 cm^2, the acceleration voltage is by far lower than the threshold of electron energy for displacement of sp^2 carbon atoms to trigger the formation of nano-onions. Nevertheless,

the subsequent developments enabled to attain 250 keV of acceleration voltage and 500 ns of pulse width at High Voltage Research Institute in Tomsk, Russia.

There will be a number of potential applications worth examining, once carbon nano-onions are produced. While some have made a "sour grapes"-like explanation that bunched agglutinates of carbon blacks are favorable for reinforcing rubber by tangling well with the polymer backbones, it is also likely that nano-dispersion of primary particles provides even a better effect due to the incomparably larger total surface area. The unique structures composed of nested fullerenes will give rise to novel properties suitable for solid-state optical limiter, solar heat storage, or in general as the substitute of graphite micropowder.

6. Production of diamond from carbon nano-onion

When carbon nano-onions are exposed to convergent electron beam irradiation under heating above 400 °C (the upper limit has not been determined) in a HRTEM, diamond cores are nucleated. Further irradiation in the temperature range 300 – 1000 °C propagates the diamond phases, converting the nano-onions into nanodiamond particles as demonstrated in Fig. 9 [10, 20]. This phenomenon was found by Banhart already in 1996 [21] (the 7th row in Table 1). If

carbon blacks are treated in this way subsequent to the crystallization into separate particles of carbon nano-onions (Fig. 2), the overall change would be the direct conversion of soot particles into much more valuable nanodiamond particles via one-pot two-stage dry reaction.

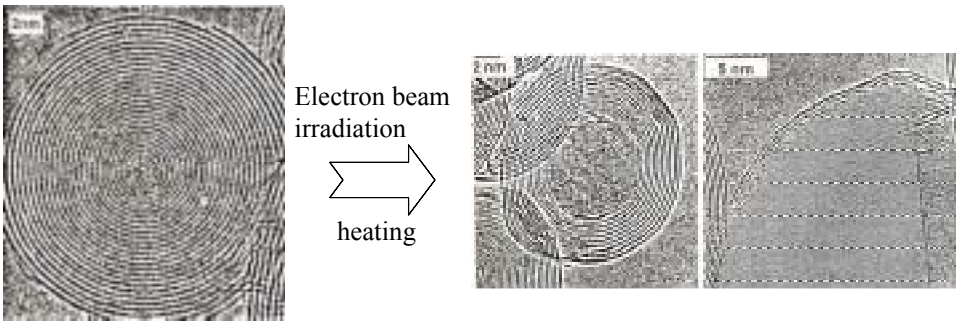

Fig. 9 Nucleation and growth of diamond cores in carbon nano-onions induced by high-voltage high-density electron beam irradiation at >400℃.

The mechanism of onion-diamond transition under the irradiation of electron beam in high vacuum is still not well understood, but represents one of the mild syntheses of diamond. Displacement of carbon atoms from onion-shells takes place by knock-on collisions of high-energy electron beam, creating interstitial-vacancy pairs. At high temperatures the vacancies are

quickly relaxed by recombination with interstitial atoms or in-plane rearrangements of the fullerene shells. This effective relaxation process plays an essential role in the onion-to-diamond transition in addition to the displacement itself. The in-plane rearrangements induced by the knock-on collisions lead to the formation of pentagon-heptagon pairs while the creation of interstitial-vacancy pairs some reduction of onion shells in size. Nano-onions undergoing these changes have more spherical shapes and smaller intershell spacing [10, 21-23], especially at inner shells, than those with the ideal configuration of $C_{60}@C_{240}@C_{540}@C_{960}@C_{1500}@\cdots@C_{60n^2}@\cdots$. This self-compression creates pressures high enough to nucleate diamond cores at the centers of the onions. Once nucleation takes place, the graphite-to-diamond transformation, a transition from a stable to a metastable phase, proceeds even at zero pressure until all the onion shells are converted due to the lower displacement threshold of graphite than that of diamond [24].

We will begin producing nanodiamond particles from carbon nano-onions as soon as the high-density high-voltage electron gun is ready. As shown in Fig. 9, buck diamond particles will be obtained as the primary products, wherein the spherical diamond particles are wrapped with a few layers of giant fullerene. The surface of such particles are susceptible to chemical reconstruction, for example

hydrogenation or functionalization. Carbon blacks have a big advantage in this production besides the low cost: various types of commercial carbon blacks have average sizes ranging between 14 and 1000 nm, hence it should be possible to produce diamond particles having different sizes, each being considerably smaller than the starting onion particles because of the higher density of diamond and the displacement of carbon atoms during the irradiation process.

Single crystals of diamond having an average diameter of 4.4±0.3 nm have been recently obtained in dispersed form from their agglutinates by stirred-media milling with micron-sized ceramic beads [15,25-26]. Crude agglutinates are produced by detonation of an oxygen-imbalanced explosive like Composition B consisting of TNT and hexogen: about one half of the soot weight that results from the incomplete combustion in the explosion is nanodiamond. This fact has been known since almost 40 years ago [27]. Thus, when the conversion of carbon blacks into diamond is realized to give double-digit-nano to submicron diamonds, we will have a whole range of diamondoid carbons starting from adamantane ($C_{10}H_{16}$), diamantane ($C_{14}H_{20}$), and higher diamondoid hydrocarbons [28] through single-digit nanodiamond by detonation (ultrananocrystalline diamond), double-digit-nano- to submicron-diamond (from carbon blacks), artificial micron-sized diamond (by the static high-pressure

high-temperature synthesis) to gem diamond larger than millimeters.

7. Production of C_{60}/C_{70} by pyrolysis

A close look at Fig. 7 indicates several possibilities of developing the furnace black process into a few interesting variations. According to our hypothesis, all primary particles of carbon blacks contain one C_{60} molecule or counter spiroid in the center (Fig. 8). This means that C_{60} can be produced using pyrolysis method at a price as low as $1/kg, if the growth process of soot can be quenched at a very early stage (the 8th row, Table 1). The possibility of pyrolytic synthesis of C_{60} was conceived in this way [29]. It would be difficult to exclude contamination of the C_{60} fraction by the smaller members of carbon nano-onions such as $C_{60}@C_{240}$ and $C_{60}@C_{240}@C_{540}$. However, these smaller onions are appealing not only as novel additions to fullerene family, but also as the starting materials for Mackay crystals or superfullerene conceived by Mackay in 1991 [39-31].

The second-generation combustion method of C_{60} synthesis developed by Howard is counted as one of the hot topics in the production of fullerenes [32]. Whereas the details of this method still remain undisclosed, the new method allegedly succeeded in entirely suppressing soot formation in contrast to the previous method, which was accompanied by large excess of soot.

Nonetheless, we note here a few essential contradictions that we found when analyzing the combustion method [33]:

(1) The whole process, which must be similar to that given in Fig. 8, takes place under extremely hostile environment of flame. Considerably high proportion of the product may have been lost by burning.

(2) Similarly, the whole complex process must be completed within a few second while in the flame. Considerably high proportion of the product may have been lost due to insufficient time.

(3) For the reactions to proceed fast enough, the flame temperature must be kept high, close or equal to 2000℃, and more and more fuel must be burnt under good supply of air, leaving less and less carbon atoms for fullerene formation.

(4) With violent oxidation reactions of combustion going on in the close vicinity of reaction zone, only a few controllable factors are available.

(5) As the result, close to 97.5% of fuel are burnt out and only 2.5% remain available for soot formation, among which only 10-20% proceed to fullerene.

On reflection, we must admit that flame is used only for the purpose of supplying heat for thermal decomposition of fuel to occur and for fullerene forming reaction sequences to proceed. However,

heat can be supplied separately from other source as well, e.g., electrical resistance under non-oxidative conditions [29].

In this regard, the furnace black process is worth examining as an archetype of pyrolytic fullerene synthesis. Fig. 1 will be employed to expound the draft. Hot fluidic heat supply, which consists of carbon dioxide and steam, is prepared by complete combustion of cheap fuel in the combusting zone colored yellow with a *proviso* that slight excess of oxygen should be left unburned in this zone for removing the surface hydrogen of raw materials sprayed afterwards. In the red-colored soot-growth region, clustering of pyrolyzed carbon atoms takes place in the order PAHs, aromers, and spiroids. In the course, the intermediate reactants must be correctly quenched in order to obtain structurally homogeneous product. Ensuing annealing process is also critical to complete the cyclization reaction and the transformation into onion-like cage structures. Finally the hot gas stream is extinguished. In order to maximize the yields of desired products, the reaction conditions must be properly modified.

The merits of pyrolytic synthesis of C_{60}/C_{70} are as follows: 1) low-cost but rational production of fullerenes, 2) low yields of by-products, and 3) many adjustable reaction conditions. Probably some of the readers will wonder why mass production is necessary, at the time when fullerenes are hardly seen in the nanocarbon market. On

the contrary, C_{60} is one of the best studied materials in the world among more than 10 million molecules investigated in chemistry, and consequently an astonishingly wide variety of applications have already been discovered and compiled [34]. Low cost of production is hence the only remaining key factor to promote applications on the industrial scale.

8. Potential synthesis of Mackay crystals

8-1. Background and synthetic design

As mentioned, according to the soot formation scheme of Fig. 7, the pyrolytic synthesis of fullerenes will be accompanied by considerable amounts of $C_{60}@C_{240}$ and $C_{60}@C_{240}@C_{540}$ as the by-products. Once the fullerene production conditions are found double- or triple-shell nano-onions will be quickly accumulated. It is desirable to have a clear perspective on the use of these by-products. Here we explore the possibility of making Mackay crystals from the small nano-onions.

Preliminary theoretical calculations suggest that $C_{60}@C_{240}$ and $C_{60}@C_{240}@C_{540}$ tend to take spherical shapes rather than polyhedral structures, therefore showing properties similar to fullerenes rather than graphite [35]. We also expect that these onions form face-centered cubic (fcc) or body-centered cubic (bcc) crystals like C_{60}

[36]. On the other hand, it has been known that C_{60} crystals transform themselves into various polymers via [2+2] cyclo-addition reactions under high pressure between 3 and 8 GPa and high temperatures as displayed in Fig. 10 [37, 38]. Among these polymers, Blank discovered a few remarkably hard carbons, even harder than diamond, formed at around 13 GPa and 670 – 820 K [39]. Rijtveld analysis was performed on one of these superhard carbons [40, 41], and the following notable features of the structure were revealed as represented in Fig. 11:

1) 3-Dimensional network is firmly constructed by forming 14 single-bond bridges from each C_{60}-derived unit.
2) An especially interesting feature is a bridge of cyclobutane ring aligned perpendicularly along *b*-axis and connecting C_{60} unit along this axis.

When Rijdveld analysis was attempted on the amorphous powder of superhard carbon, an unusually small inter-C_{60} unit distance, about 0.86 nm, was found. Incidentally this short distance coincided with in inter-C_{60} unit distance in the optimized geometry of structure **B** of Fig. 12, which depicts the first three C_{120} intermediate structures, hand-generated in a study on the likely course of Stone-Wales rearrangement sequence starting from [2+2] C_{60} dimer (**A**) [42]. When the optimized structure **B** was fit to the subsequent Rijdveld analysis,

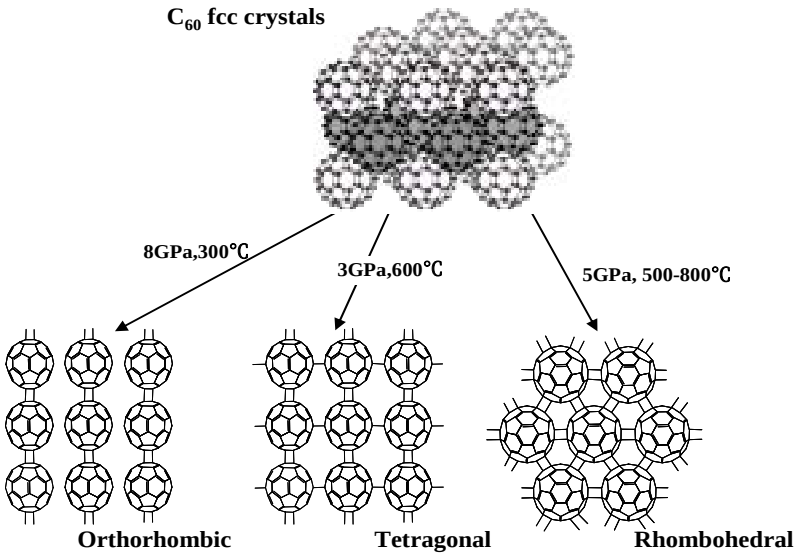

Fig. 10. 1- and 2-dimensional [2+2] polymers obtained by high-temperature high-pressure treatments of C60 crystals.

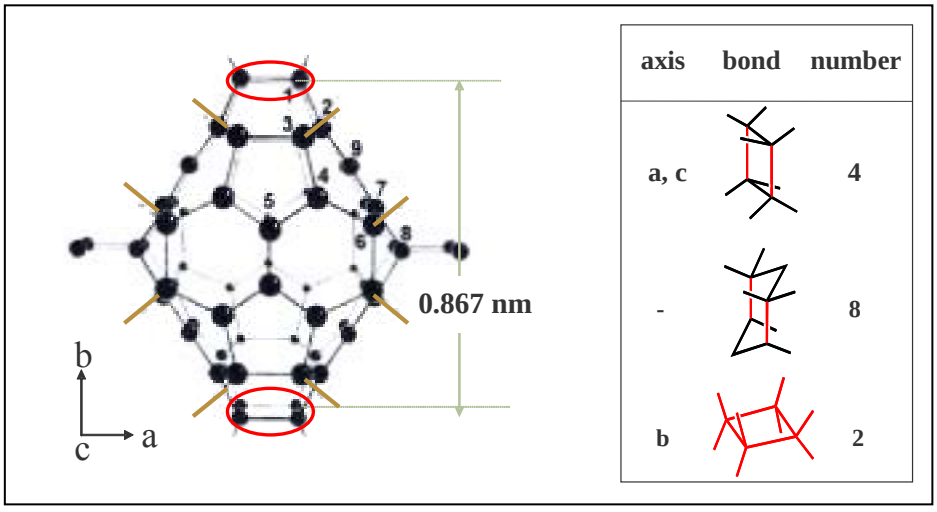

Fig. 11. C60-derived asymmetric unit with its bonding patterns with neighboring units in the body-centered orthorhombic lattice of the superhard 3-dimensional polymer of C60.

the crystal structure of the superhard carbon could be solved with a

satisfactory fitness level.

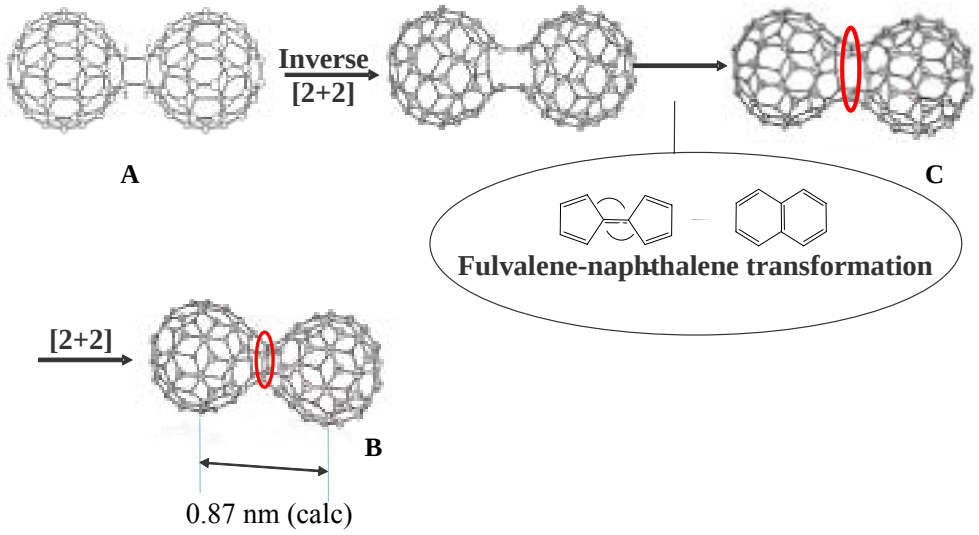

Fig. 12 Three-step transformation pathway of [2+2] C60 dimer (**A**) into a fused structure (**B**), which has been found in the superhard C60 3D-polymer having double-sided cyclobutane bridges along *b*-axis. The pathway is derived by hand.

Upon inspection of the resulting crystal structure, we felt that a key factor contributing to the particularly high hardness of this carbon must be those strong bridges of double-sided cyclobutane ring formed along *b*-axis in each C_{60}-derived unit. According to this assumption, even harder carbon materials will be obtained if 3-dimensional C_{60} polymers having wide and stronger bridges were made.

Later, we wrote a program to deduce the shortest Stone-Wales rearrangement pathways starting from [2+2] C_{60} dimer and reaching

the shortest carbon nanotube C_{120} (**24**, Fig. 13) [43]. In this long sequence we found a number of intermediates having thick and wide bridges as mentioned above, but we were puzzled to realize that the structure **B** with double-sided cyclobutane ring in the center was missing in this route. In our previous hand-driven pathway (Fig. 12), the intermediate **C**, which corresponds to the molecule **4** in Fig. 13, is the precursor of **B**. However, **4** changed into **5**, then into **6** and so on, never yielding **B**. The reason is two-fold. First, structure **B** is a dead end, from whence there is no Stone-Wales pathway to evolve into stable isomers. The other reason is that in crystal C_{60} molecule is

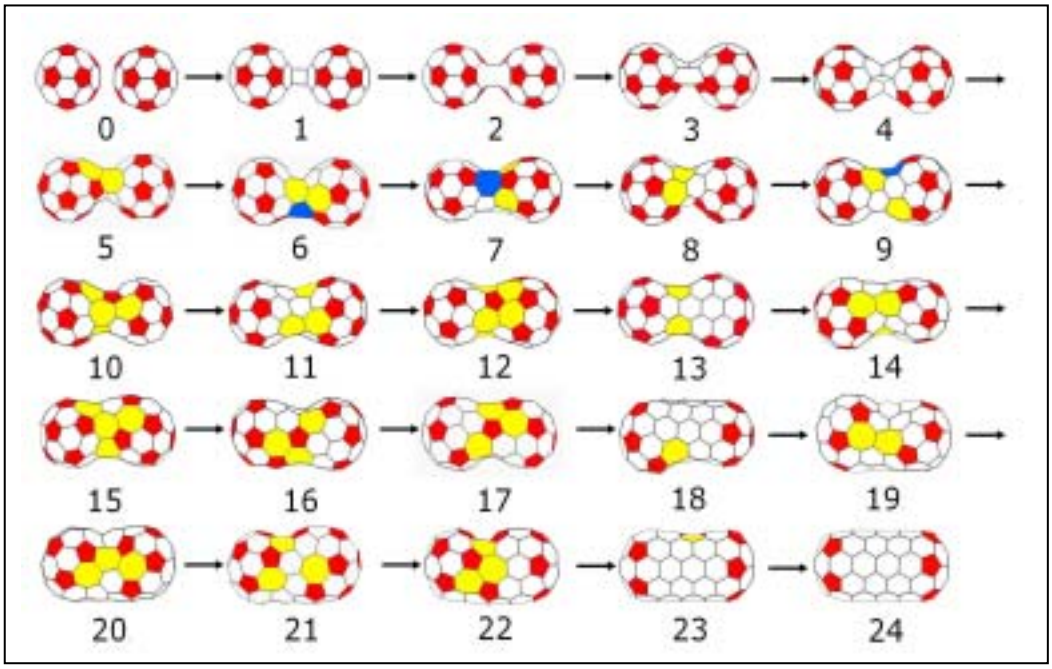

Fig. 13. Computer-generated shortest pathway from [2+2] C60 dimer (1) to the shortest C120 carbon nanotube (**24**) through Stone-Wales rearrangements. Hexagons, pentagons, heptagons, and octagons are colored white, red, yellow, and blue, respectively.

bonded with the other neighboring C_{60} units; hence only a few carbon atoms are left for bridging even at this early stage. In other words, we need fullerenes much larger than C_{60} in order to create still harder carbon materials wherein it is desirable that each fullerene unit is bonded to at least six neighboring fullerene units by thick and strong bridges.

Giant fullerenes like C_{100} are, however, hardly available. Hereby we believe that $C_{60}@C_{240}$ and $C_{60}@C_{240}@C_{540}$ can be potential candidates for the superhard materials. Having almost spherical outershell, these fullerenes will form a similar crystal of multi-dimensional polymers by [2+2] addition reaction like C_{60} upon heating the crystals under high pressure. At some point during the evolution of inter-unit bridges, the shrinking outershell will exert high pressure upon inner shells and eventually destroy them so that many carbon atoms will become available for constructing stronger, wider and thicker bridges. The final result of high-pressure high-temperature treatment of these multi-layered fullerene crystals will be hard carbons having jungle gym skeleton made of wide bridges and fullerene-like joints. Strain will be minimized by Stone-Wales rearrangements in the network to create smooth curved surface having negative Gaussian curvatures. Then, we have Mackay crystals.

8-2. Predicted properties of Mackay crystals

As mentioned above, Mackay crystals (Table 3) [30, 31] are novel carbon structures conceived by Mackay as the topological counterpart of C_{60}. The most prominent feature of the crystals is that any points on the curved surfaces are saddle points with negative Gaussian curvatures ($K < 0$). Whereas no surface having constant negative K converges in the real space, periodically curved surfaces are possible with varying K. Some of such surfaces were discovered in the 19th century by Schwarz, and named Schwarz surfaces. In analogy with mineral crystals, they are often called Schwarzites. Patchwork of graphitic tiles consisting of 4- to 8-membered rings onto the surfaces of Schwarzites gives the Mackay crystals. We have also used a similar strategy to generate a hypothetical superdiamond structure [44-46].

Unlike the times of Schwarz and Mackay, the practical syntheses of these crystals are actually forthcoming as argued in the precedent section. A sketch of synthetic scheme for a Mackay crystal based on the simplest p-type Schwarzite is depicted in Fig. 14. Numerous applications can be proposed for a Mackay crystal in view of its remarkable characteristics predicted, like superhardness, nano-porosity, and novel electronic structures inherent to the unique continuous

Table 3 Topological comparison between C_{60} and Mackay crystal.

comparative items	C_{60}	Mackay crystals
Gaussian curvature	K>0 constant	K≤0 variable
average of curvature	H>0 constant	H=0 minimal surface
singularity	center point	omphalos
symmetry	I_h	repeating unit of p-type is O_h
primary factor for discreteness	5-,6-,(7-) membered rings	6-,7-,8-membered rings 4-,9-,10-membered rings are also possible
pores	no	yes p-type has 6 pores per unit cell
number of C	60	∞ crystal
structural rigidity	high	?
thermodynamic stability	high energy minimum	unknown low energy minimum?
spatial division by surface	uneven division	equivalent division zeolite-like
surface shape	spherical	Schwarz surface p-, d-, g-types etc.
synthesis	relatively easy	possible?

network structure. Especially, there are uncountable applications of superhard materials like diamond. It would be a wonderful material of boring drills or cutters for the investigation of underground. Not only exploration of natural resources in relatively remarkable

characteristics predicted, like superhardness, nano-porosity, and novel electronic structures inherent to the unique continuous network structure. Especially, there are uncountable applications of superhard materials like diamond. It would be a wonderful material of boring drills or cutters for the investigation of underground. Not only exploration of natural resources in relatively shallow underground, say down to 5 km, but also collecting geological informations of somewhat deeper underground like 30 km, are evidently important and rewarding subjects of research. Another interesting aspect of Mackay crystal may be worthwhile a brief mention here. If heptagons and/or octagons, essential for the negative curvatures of Schwarzites,

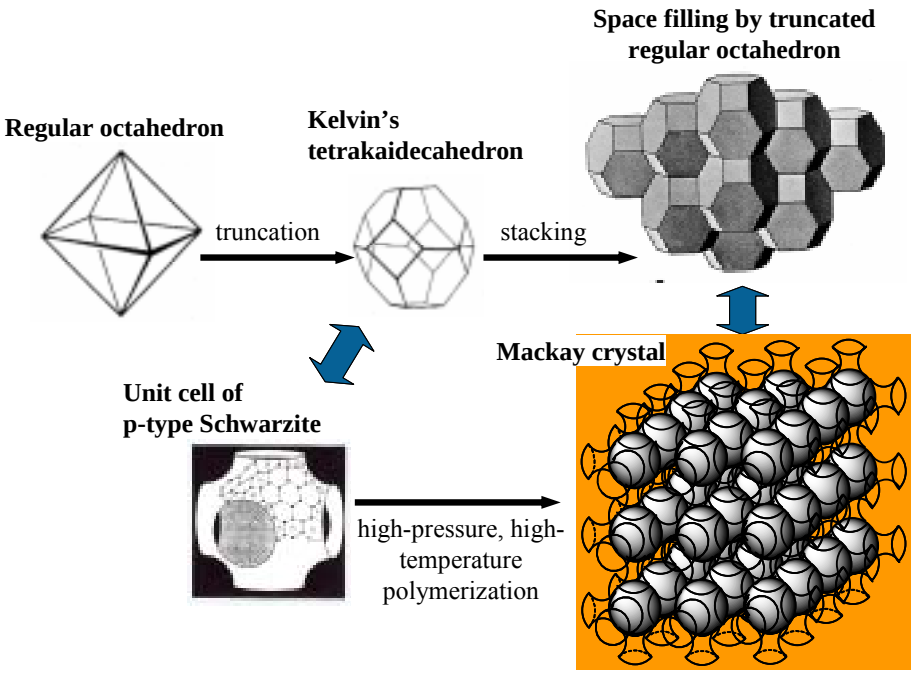

Fig. 14 Mackay crystal consisting of p-type Schwarzite.

are completely oriented in the infinite translational repetition of the unit cells in Mackay crystal, they might cause strong ferromagnetism [47].

9. A tentative proposal for carbon blacks-derived nano-carbon industries

Among the conceivable nano-carbon industries related to carbon blacks, those plans that are already taking concrete shape are presented in Fig. 15. The two rows on the lower half signify direct utilization of carbon blacks, while the other two will need some modification in the reactor system of furnace blacks. All these plans were given solid

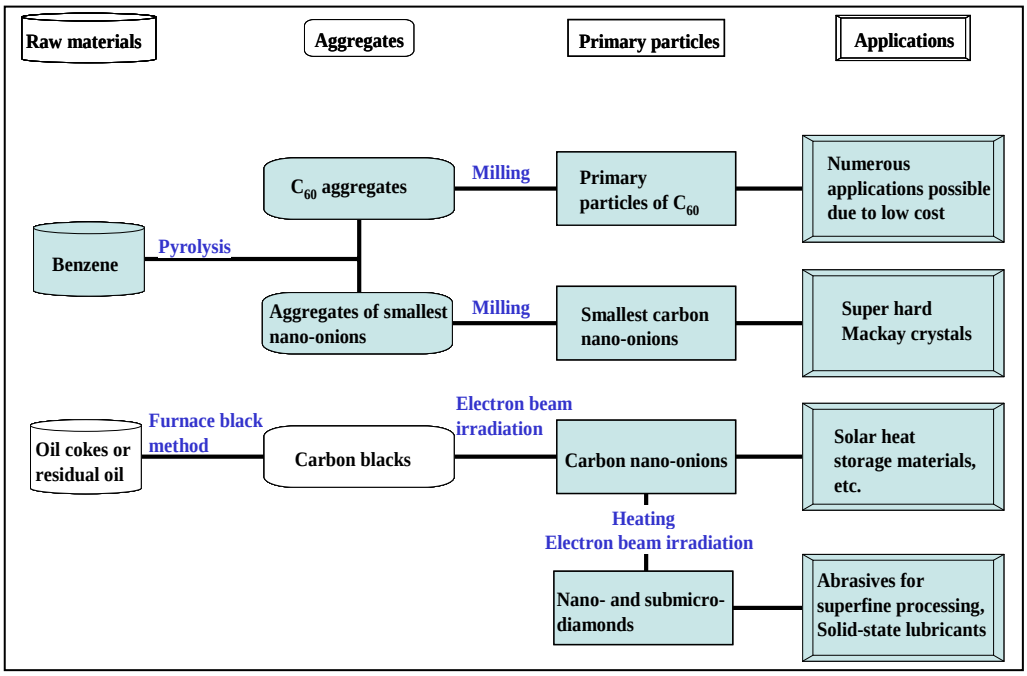

Fig. 15. Nanocarbon industry that uses carbon blacks and their precursors as the raw materials.

background ever since we reconfirmed Kroto's original proposal that primary particles of soot are defective carbon nano-onions (Fig. 8). We still have a long way to go, and actually the important phases discussed in the sections 5 and 6 have been examined only in very preliminary experiments. However, it is delightful to look forward to the new materials and to what they will bring in our lives.

Acknowledgments

E. O. thanks receipt of NEDO Grant, 2004-2007, and financial support from Futaba Corporation, 2001-2004.

References

1. http://www.nano.gov/
2. E. Ōsawa (Ed), *Perspectives of Fullerene Nanotechnology*, Kluwer Academic, Dordrecht, Netherlands (2002).
3. A. M. Thayer, *C&EN*, 83 (2005) 17.
4. J.-B. Donnet, R. C. Bansal and M.-J. Wang, (Eds.), *Carbon Blacks, Second Edition*, Dekker, New York (1993).
5. T. Kato, G. Akiyama, Y. Akiyama, T. Nakahara, T. Hayasaka, B. Hoshino and T. Yamasaki (Eds.), *Carbon Black Handbook, Third Edition*, Carbon Black Association, Tokyo (1995).

6. M. Ozawa, H. Goto, M. Kusunoki and E. Ōsawa, *J. Phys. Chem. B.* 106 (2002) 7135.

7. R. E. Franklin, *Proc. Roy. Soc.* A209 (1951) 196.

8. H. R. Kroto, K. Prassides and R. Taylor, D. R. M. Walton, in: *The Chemical Physics of Fullerenes 10 (and 5) Years Later*, W. Andreoni (Ed.), p. 3, Kluwer Academic, Dordrecht, Netherlands (1995).

9. D. Ugarte, *Nature* 359 (1992) 707.

10. F. Banhart, *Rep. Prog. Phys.* 62 (1999) 1181.

11. E. D. Obraztsova, M. Fujii, S. Hayashi, V. L. Kuznetsov, Yu. V. Butenko and A. L. Chuvilin, *Carbon* 36 (1998) 821.

12. M. Yoshida, E. Ōsawa, *Fullerenes Sci. Technol*. 1 (1993) 55.

13. K. H. Homann, *Angew. Chem. Int. Ed*. 37 (1998) 2434.

14. E. Ōsawa, K. Aigami, N. Takaishi, Y. Inamoto, Y. Fujikura, Z. Majerski, P. v. R. Schleyer and E. M. Engler, *J. Am. Chem. Soc.* 99 (1977) 5361.

15. A. Krüger, F. Kataoka, M. Ozawa, T. Fujino, Y. Suzuki, A. E. Aleksenskii, A. Ya. Vul' and E. Ōsawa, *Carbon* in press.

16. Manuscript in preparation.

17. G. A. Mesyats, *Explosive Electron Emission*, URO-Press,

Ekaterinburg, Russia (1998).

18. P. Raharjo, H. Wada, Y. Nomura, G. E. Ozur, D. I. Proskurovsky, V. P. Rotshtein and K. Uemura, Proceedings of the 6th International Conference on Modification of Materials with Particle Beams and Plasma Flows, pp. 679-682, Tomsk Tech. Univ., Tomsk, Russia (2002).

19. A. Okada, Y. Uno, N. Yabushita, K. Uemura and P. Raharjo, International Conference on Large Edge Manufacturing in the 21st Century, pp. 1023-1028, Niigata Univ., Niigata, Japan (2003).

20. M. Zaiser and F. Banhart, *Phys. Rev. Lett.* 79 (1997) 3680.

21. F. Banhart and P. M. Ajayan, *Nature* 382 (1996) 433.

22. H. Terrones and M. Terrones, *J. Phys. Chem. Solids*, 58 (1997) 1789.

23. K. R. Bates and G. E. Scuseria *Theor. Chem. Acc.* 99 (1998) 29.

24. M. Zaiser, Y. Lyutovich and F. Banhart, *Phys. Rev. B*, 62 (2000) 3058.

25. E. Ōsawa, in: *Synthesis, Properties and Applications of Ultrananocrystalline Diamond*, D. M. Gruen, O. A. Shenderova and A. Ya Vul' (Eds.), Springer, Dortrecht,

Netherland (2005).

26. E. D. Eidelman, V. I. Siklitsky, L. V. Sharonova, M. A. Yagovkina, A. Ya. Vul', M. Takahashi, M. Inakuma and E. Ōsawa, *Diamond & Rel. Mater*. submitted for publication.

27. O. A. Shenderova, V. V. Zhirnov and D. W. Brenner, *Crit. Rev. Solid State Mater. Sci.* 27 (2002) 227.

28. J. E. Dahl, S. G. Liu, R. M. K. Carlson, *Scienceexpress*, 2002, 10782391.

29. E. Ōsawa, *Japanese Kokai Patent* 2005-8500, *Appl.* 2003-177403.

30. A. L. Mackay and H. Terrones, *Natur*e, 352 (1991) 762.

31. A. L. Mackay and H. Terrones, *Phil. Trans. R. Soc. Lond. A* 343 (1993) 113.

32. J. B. Howard and D. F. Kronholm, 2003 Nanotechnology Forum, National Taiwan University, Taipei, Taiwan.

33. M. Ozawa, P. Deota and E. Ōsawa, *Fullerene Sci. Technol*. 7 (1999) 387.

34. K. M. Kadish and R. S. Ruoff (Eds.), *Fullerenes: Chemistry, Physics and Technology*, John Wiley & Sons, New York (2000).

35. Unpublished results.

36. M. S. Dresselhaus, G. Dresselhaus and P. C. Eklund, *Science of Fullerenes and Carbon Nanotubes*, Academic Press, San Diego, Chapt. 7 (1995).

37. Y. Iwasa, T. Arima, R. M. Fleming, T. Siegrist, O. Zhou, R. C. Haddon, L. J. Rothberg, K. B. Lyons, H. L. Carter, Jr., A. F. Hebard, R. Tycko, G. Dabbagh, J. J. Krajewski, G. A. Thomas and T. Yagi, *Science* 264 (1994) 1570.

38. M. Nuñez-Regueiro, L. Marques, J.-L. Hodeau, O. Béthoux and M. Perroux, *Phys. Rev. Lett.*, 74 (1995) 278.

39. V. Blank, S. Buga, G. Dubitsky, N. Serebryanaya, M. Popov and V. Prokhorov, in: ref. 2, pp. 223-233.

40. L. A. Chernozatonskii, N. R. Serebryanaya and B. N. Mavrin, *Chem. Phys. Lett.* 316 (2000) 199.

41. N. R. Serebryanaya and L. A. Chernozatonskii, *Solid State Commun*. 114 (2000) 537.

42. S. Ōsawa, E. Ōsawa and Y. Hirose, *Fullerene Sci. Technol*. 3 (1995) 565.

43. H. Ueno, S. Ōsawa, E. Ōsawa and K. Takeuchi, *Fullerene Sci. Technol*. 6 (1998) 319.

44. E. Ōsawa, M. Yoshida and M. Fujita, *MRS Bull*. 19 (1994) 33.

45. M. Fujita, T. Umeda, M. Yoshida and E. Ōsawa, *Synth.*

Metals 71 (1995) 1897.

46. M. Fujita, M. Yoshida and E. Ōsawa, *Fullerene Sci. Technol*. 3 (1995) 937.

47. T. Makarova, B. Sundqvist, R. Höhne, P. Esquinazi, Y. Kopelevich, P. Scharff, V. A. Davydov, L. S. Kashevarova and A. V. Rakhmanina, *Nature* 413 (2001) 716.

Figure legends

Fig. 1 Pyrolysis furnace for carbon blacks. Classical process produces chemically pure carbon which turned to be a sort of fullerene.

Fig. 2 Crystallization of carbon black structure by intensive electron beam bombardment (JEOL, JEM-2010 at 200 keV, ~150 A/cm^2) onto Toka Black #8500F, claimed to have an average diameter of 14 nm in the primary particles. *a*) Pristine structure shows numerous defects and ambiguous grain boundaries. *b*) After irradiation for 20 min at this spot spherical contours and inner-layers of carbon nano-onions clearly appeared.

Fig. 3 Reversible transformation between the intermediate spiral particle (spiroid) *a*) and the carbon nano-onion *b*) observed under electron beam irradiation onto primary particles of carbon blacks.

Fig. 4 Molecular and numerical (inset) models of a 3-dimensional double-layer spiral particle (spiroid), C_{300}.

Fig. 5 Presumed reaction scheme of the reversible transformation between a double-layer carbon spiroid, C_{300}, and a double-shell carbon nano-onion $C_{60}@C_{240}$. Cleavage of onion-shell starts at weak C-C bonds at structural defects, fused pentagons, etc., and prompts interlayer valence-bond isomerization

Fig. 6 Chemical transformations in the incomplete combustion process of hydrocarbon proposed by Homann. The first intermediates PAH polymerize into *syn*-dimer and other oligomers (aromers) but only the syn-dimer of thirty-carbon PAH is transformed into C_{60}, while all the other aromers grow into soot.

Fig. 7 Unified mechanism of formation/growth of soot, C_{60} and

nano-onions. Some PAHs and only one aromer out of numerous structures are depicted as examples.

Fig. 8 Model of core agglutinate of a high-structure carbon black. Primary particle are believed to contain C_{60} or its congener in its centre. Outer layers are merged into large deformed and defective graphene sheets that hold the assembly of primary particles which are highly defective multi-shell fullerenes or its spiroidal counterpart.

Fig. 9 Nucleation and growth of diamond cores in carbon nano-onions induced by high-voltage high-density electron beam irradiation at >400 ℃.

Fig. 10 1- and 2-dimensional [2+2] polymers obtained by high-temperature high-pressure treatments of C_{60} crystals.

Fig. 11 C_{60}-derived asymmetric unit with its bonding patterns with neighboring units in the body-centered orthorhombic lattice of the superhard 3-dimensional polymer of C_{60}.

Fig. 12 Three-step transformation pathway of [2+2] C_{60} dimer (**A**) into a fused structure (**B**), which has been found in the superhard C_{60} 3D-polymer having double-sided cyclobutane bridges along *b*-axis. The pathway was derived by hand.

Fig. 13 Computer-generated shortest pathway from [2+2] C_{60} dimer (**1**) to the shortest C120 carbon nanotube (**24**) through Stone-Wales rearrangements. Hexagons, pentagons, heptagons, and octagons are colored white, red, yellow, and blue, respectively.

Fig. 14 Mackay crystal consisting of p-type Schwarzite

Fig. 15 Nanocarbon industry that uses carbon blacks and their precursors as the raw materials.

Fig. 1 Pyrolysis

List of Tables